A novel 3D segmentation method of the lumen from intravascular ultrasound images

Alexandrescu, Ionut; Cheriet, Farida; Delorme, Sébastien

Publisher's version / Version de l'éditeur:
https://doi.org/10.1007/978-3-540-74260-9_84
Image Analysis and Recognition: 4th International Conference, ICIAR 2007, Montreal, Canada, August 22-24, 2007. Proceedings, Lecture Notes in Computer Science; no. 4633, pp. 949-960, 2007

A Novel 3D Segmentation Method of the Lumen from Intravascular Ultrasound Images

Ionut Alexandrescu[1], Farida Cheriet[1,2] and Sébastien Delorme[3]

[1] Institute of Biomedical Engineering, [2] Department of Computer Engineering.
École Polytechnique de Montréal, Campus de l'Université de Montréal, 2500, chemin de Polytechnique, Montréal, QC, H3T 1J4.
[3] Industrial Materials Institute, 75 de Mortagne, Boucherville, QC, J4B 6Y4
{ionut.alexandrescu, farida.cheriet, @polymtl.ca; sebastien.delorme@cnrc-nrc.gc.ca}

Abstract. In this paper a novel method that automatically detects the lumen-intima border on an intravascular ultrasound sequence (IVUS) is presented. First, a 3D co-occurrence matrix was used to efficiently extract the texture information of the IVUS images through the temporal sequence. By extracting several co-occurrence matrices a complete characterization feature space was determined. Secondly, using a *k*-means algorithm, all the pixels in the IVUS images were classified by determining if they belong to either the lumen or the other vessel tissues. This enables automatic clustering and therefore no learning step was required. The classification of the pixels within the feature space was obtained using 3 clusters: two clusters for the vessel tissues, one cluster for the lumen, while the remaining pixels are labeled as unclassified. Experimental results show that the proposed method is robust to noisy images and yields segmented lumen-intima contours validated by an expert in more than 80% of a total of 300 IVUS images.

Keywords: IVUS segmentation, 3D co-occurrence matrix, *k*-means classification, swap heuristics, texture analysis.

1 Introduction

Intravascular ultrasound (IVUS) is a catheter-based imaging technique that enables clinicians to see blood vessels cross-sections from inside out (*see figure 1*), including the blood flowing through the lumen of the vessel, and the three layers of the vessel wall (intima, media and adventitia). Coronary arteries are the most frequent imaging target for IVUS. This technology is used in coronary arteries to assess the spatial distribution of atheromatous plaque (also known as atherosclerosis) in the coronary tree. Plaque buildup causes stenosis – a narrowing of the artery – and reduces blood flow. IVUS is more precise than angiography to determine the degree of stenosis because of image resolution, and because angiographic images are just 2D projections of a 3D shape which is not necessarily symmetrical. IVUS is often used as a research tool to improve atherosclerosis diagnosis, treatment planning and assessment of treatment efficiency, at the cost of lengthy manual segmentation of the lumen-intima and the media-adventitia borders. Fast and automatic IVUS image segmentation would improve the clinical usefulness of IVUS.

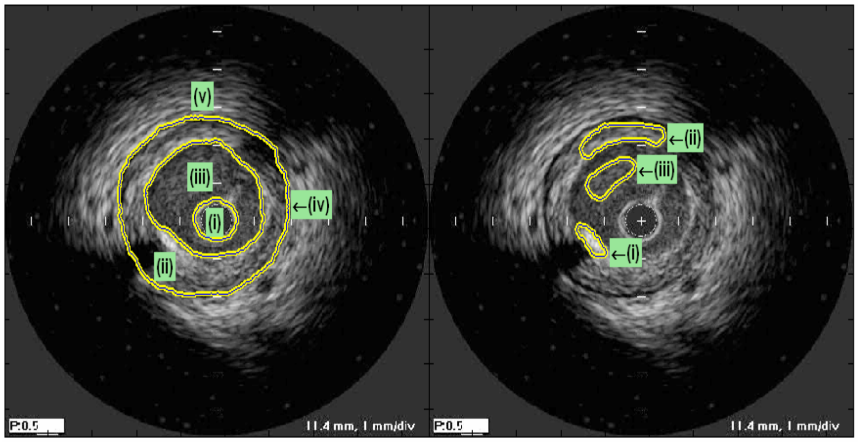

Fig. 1. (*Left*) A traditional IVUS image illustrating three layers around the lumen *(iii)*: the intima *(ii),* the media (iv) and the adventitia (v).The IVUS catheter is in the middle (i) (*Right*) Plaque composition consists of fibro-lipid*(ii)* and calcium deposits *(i)*. The lumen is the blood (*iii*).

Much research work has been done on IVUS segmentation, including the development of several methods to obtain the desired borders. In [1] combination of several techniques is used by minimizing a global cost function calculated using: (i) the intensity patterns learned from examples, (ii) statistical proprieties of ultrasound and (iii) area homogeneity. This technique requires the construction of patterns from manually segmented images. This stage is very difficult to accomplish properly due to the large variability of IVUS images from one patient to another and the intensity discontinuities between the lumen and the intima. An automatic segmentation approach using a level set (fast marching method) is presented in [2, 3]. To find the initial parameters of the level set, Rayleigh distributions are searched in the histogram of the sequence of images. However, this method was only tested on images obtained on femoral arteries, therefore containing less motion blur and being of better quality when compared to coronary IVUS images.

Popular methods rely on both texture analysis and classification of the IVUS images in order to segment the various vessel borders. Local Binary Patterns [4, 5], 2D co-occurrence matrices [5, 6], or both methods [7] have been used mainly for texture analysis. An analysis of cumulative moments was used in [5], and a fuzzy *k*-means approach is used in [8] where several clusters are defined for the various layers of the vessel. All these methods are implemented in two dimensions and hence the results are calculated from a single static image only. Once texture characterization is finalized, a second phase is implemented that consists in the use of a classifier in order to find the desired vessel border. In [4, 5], an Adaboost or a *k*-nearest neighbors classification is used to classify the pixels of an IVUS image. These two methods require a training phase, which requires a large image database in order to be efficient and effective. In [6, 7], IVUS segmentation is accomplished using a deformable contour analysis, such as Snakes, in combination with a texture analysis procedure. This technique assumes that the extraction of characteristics behaves like a filter in order for the contours to evolve and converge correctly, which is not always the case with noisy images.

This paper presents a novel approach to automatically find the lumen-intima border using a 3D co-occurrence matrix feature extraction, and a *k*-means classifier on IVUS coronary images. A major advantage of the proposed method is that it does not involve any supervised training and it exploits the temporal information contained in the IVUS sequence.

2 Methodology

The proposed method is mainly based on a 3D texture analysis performed on a specified number of IVUS images. Those images are recorded at 30 fps with an ultrasound catheter pulled back at a controlled speed of 0.5 mm/s, over a few minutes. In coronary arteries, the heart produces significant motion and deformation of the artery cross-section between each heart beat. Hence, the temporal information of the IVUS sequence is taken into account. First, the three dimensional co-occurrence matrices were computed to extract 3D characteristics. Secondly, the classification was performed using a *k*-means algorithm with a slight modification. A hybrid method between Lloyd and a heuristic swap was used [10, 11], to avoid local minima during the optimization process. Finally, a three cluster *k*-means was used: one cluster represents the lumen and the two others represent the artery itself. The unclassified pixels were identified and then the border was detected consequently.

2.1 Preprocessing

An IVUS film lasting several minutes is usually composed of a few thousand images. The segmentation process can be speeded up by segmenting a subsample of the images, and interpolating between the found contours. By extracting images synchronized with the electrocardiogram (ECG), one image for each cardiac cycle, the motion blur due to the cycle-to-cycle variation of blood pressure was partly eliminated, while reducing the number of total images to segment in a sequence. To make the extraction of characteristics optimal, the images were transformed into polar coordinates by using a bi-cubic interpolation (*See Figure 2*). When the transformation is made, the image artifacts such as the calibration markers visible on every image were eliminated by a thresholding fallow by an interpolation procedure. The catheter, which appears as a black band between two white bands on the polar images, was also removed by a histogram analysis followed by a thresholding procedure.

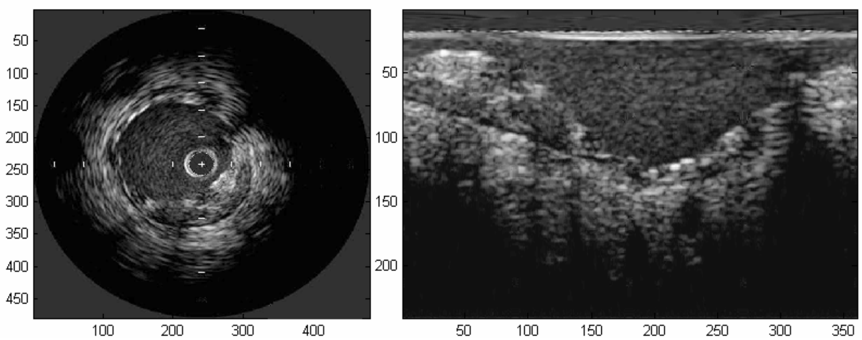

Fig. 2. (*Left*) Original IVUS image. (*Right*) IVUS image transformed in polar coordinates using bi-cubic interpolation.

2.2 3D Co-occurrence matrices

Co-occurrence matrices [12] are a statistical tool which allows the extraction of second-order texture information from an image. The frequency between pairs of pixels i and j of various gray scales, to a certain shift, is calculated and placed in a matrix C. The matrix of co-occurrence $C\ (i,j,d,\theta)$, for a radius r and an angle θ is defined by:

$$C(i,j,d,\theta)=\left|\{(r,c)\mid I(r,c)=i \text{ and } I(r+d\cos(\theta),c+d\sin(\theta))=j\}\right| \quad (1)$$

Matrix C indicates the number of times the value of pixel i is in relation to the value of pixel j in a space relation. This space relation is described by r and θ which define respectively the distance and the orientation between the two pixels. For one 2D image, matrix C is a square matrix representing the number of gray scales in the image.

In this paper, 3D co-occurrences matrices for volumetric data [9] were used. These 3D matrices are able to identify the space dependence of the gray scales through the IVUS sequence. They are similar to the 2D matrices but the calculation of the C matrix is made from a cubic window rather than a square window. Therefore, the space shift between two pixels will be in three dimensions. Equation (1) becomes:

$$C(i,j,d,\theta,\phi)=\left|\{(r,c)\mid I(r,c)=i \text{ and } I(r+d\cos(\theta)\sin(\phi),c+d\sin(\theta)\sin(\phi))=j\}\right| \quad (2)$$

Once matrix C is found, the analysis is similar to the 2D case. The co-occurrence matrix can be normalized with respect to the characteristics to be extracted. These characteristics are presented in table 1:

TABLE I

CO-OCCURRENCE MATRICES CHARACTERISTICS

Characteristic	Formula	Characteristic	Formula
Energy	$\sum_{i=1}^{M}\sum_{j=1}^{L}\left(N(i,j)^2\right)$	Entropy	$-\sum_{i=1}^{M}\sum_{j=1}^{L}\left(N(i,j)\log N(i,j)\right)$
Shade	$\sum_{i=1}^{M}\sum_{j=1}^{L}\left(((i-\mu_i)+(j-\mu_j))^3 N(i,j)\right)$	Inverse Difference Moment (IDM)	$\sum_{i=1}^{M}\sum_{j=1}^{L}\left(\frac{N(i,j)}{1+(i-j)^2}\right)$
Promenance	$\sum_{i=1}^{M}\sum_{j=1}^{L}\left(((i-\mu_i)+(j-\mu_j))^4 N(i,j)\right)$	Inertia	$\sum_{i=1}^{M}\sum_{j=1}^{L}\left((i-j)^2 N(i,j)\right)$
Correlation	$\sum_{i=1}^{M}\sum_{j=1}^{L}\frac{(i-\mu_i)(j-\mu_j)N(i,j)}{\sigma^2}$	Rayleigh density	$\frac{\mu}{\sigma}$

N(i,j) - Normalized co-occurrence matrix.
M, L - Number of columns and lines of the matrix N.
μ_i - Vector representing the mean of each column.
μ_j - Vector representing the mean of each line.
μ - Mean of the matrix N.
σ - Standard deviation of the matrix N.

To extract the characteristics from an image, the above 8 characteristics are calculated on cubes centered on each pixel of the image. The size of the cube must be chosen as well as the angles of the *C* matrix. There are 13 possible pairs of angles, represented by the following directions: d(1,0,0); d(0,1,0); d(0,0,1); d(1,1,1); d(-1,1,1); d(1,-1,1); d(1,1,-1); d(0,1,1); d(1,0,1); d(1,1,0); d(1,0,-1); d(0,1,-1); d(-1,1,0)[9] (*see Figure 3*) .

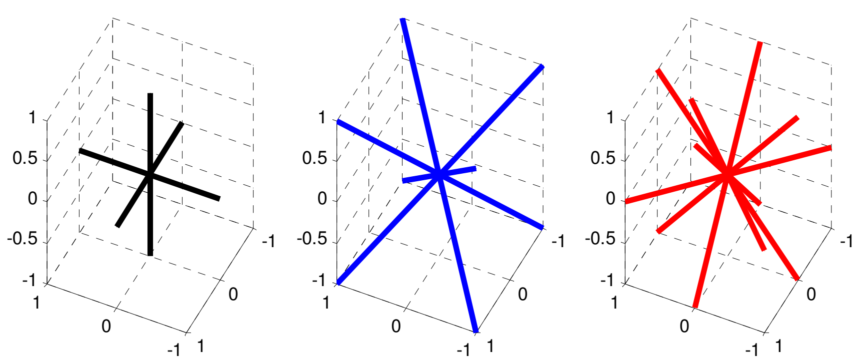

Fig.3. The 13 directions given by the possible angles of the co-occurrence matrices.

2.3 Features Space

A features space (*see figure 4a*) was created using the 3D co-occurrence matrices. Several parameters values must be selected: cube size, direction (*angle*) of the calculation of the co-occurrence matrices, and number of characteristics to be extracted from the matrices.

Since the algorithm needs images before and after the image being analyzed, the first and the last images were analyzed by extrapolating the border (*see figure 4b*). For the same reason, a part of the top of the image and a part of bottom of the image cannot be analyzed. Selecting the size of the cube to be smaller than the lumen enables the contour between the lumen and the intima to be inside the part to be analyzed. With respect to the angle, a circular padding is used to fill the missing region. Laslty, a principal components analysis (PCA) [13] is performed to reduce the space dimension by eliminating the correlation between the characteristics.

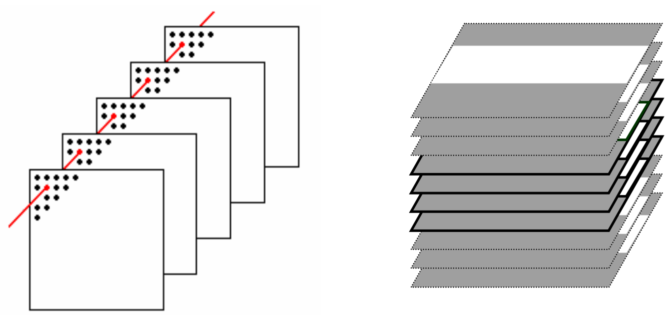

Fig. 4. *(a left)* For each pixel we create a feature space. *(b right)* The characteristics of the images in stipple and gray can't be extracted.

2.4 k-means classifier

The goal of the classifier is to associate each given data from a distribution to a cluster. The *k*-means classifier has the advantage of being completely automatic; therefore it does not need any learning phase. Once the number of clusters is specified, the classifier finds the centers of each one. The distribution can be of any dimension. The hybrid *k*-means, used in this paper, is a combination method between Lloyd method and a heuristic swap [10, 11].

This method starts by generating an initial solution and then tries to improve it by using the Lloyd algorithm followed by a heuristic swap algorithm. This approach allows the optimization process to avoid local minima. The Lloyd algorithm, also known as *k*-means algorithm, takes initial centers and calculates the neighborhood for each center. Each initial center then moves towards the centroid of the neighborhood until satisfaction of a convergence criterion. This algorithm converges towards an optimal solution, which could be a local minimum.

At this point, the swap heuristic algorithm selects a set of k initial centers S from the potential centers, R. The algorithm then tries to constantly improve the solution by removing a center $s \in S$ and by replacing it with another $s' \in R - S$. Let $S' = S - \{s\} \cup \{s'\}$ be the new set of centers. If the modified solution has a smaller distortion than the existing solution then S is replaced by S', otherwise S doesn't change. This swap is done until there aren't any more changes in the distortion after several swaps. The decision to apply several steps of the Lloyd algorithm is based on the amount of update from one step to another. This quantity is defined by determining an empiric threshold value. The new solution is accepted if it is better than the old one [10, 11].

By using the algorithm we are able to find the centers of the clusters from a given distribution. In our case, the distribution is composed of pixels characteristics obtained from the 3D co-occurrence matrices. Once the centers of the clusters are found, the pixels are classified according to the three clusters. As mentioned previously, one cluster represents the lumen and the two others represent the remaining vessel structures. The vessel has several textures representing the different tissues which are regrouped in the two classes. During the classification, the pixels which are at a similar distance from the lumen center to one of the vessel centers are identified as unclassified.

2.5 Postprocessing

After classification, the pixels are assigned to four classes: those who belong to the lumen, those who belong to the two vessel clusters, and the uncertain ones. A segmented image of this is produced by assigning for each class a number n such that $n = [0, 3]$. This image is filtered with a "closing" morphological filter to eliminate isolated pixels [14]. The two classes of the vessel are merged so that the final segmented image has only three classes, representing the lumen, the vessel, and an uncertain region between them. Then, the lumen-vessel border is found in the center of the uncertain area. The border is then transformed from polar coordinates back into the format of the initial IVUS image. In order to correct errors that might occur during this postprocessing step, an active contour methods can be used, such as Snakes [15] with an external energy taken from the gradient of the original image filtered with a Gaussian filter.

2.6 Evaluation

IVUS images obtained with a rotating catheter, at 20 MHz of ultrasound frequency, are used to evaluate the proposed method. The images have an original size of 480 x 480 pixels and are converted in polar coordinates (r, θ), having a size of 360 pixels along θ and 240 pixels along r. Eight characteristics were extracted for several sizes of cubes with various angle directions. A 17x17x17 cube was selected with characteristics calculated in the following directions: d(1,1,1); d(1,0,0); d(0,1,0); d(0,0,1); d(1,1,0); d(0,1,1); d(1,0,1); and a 9x9x9 cube, with the characteristics calculated in the directions: d(1,1,1); d(1,0,0); d(0,1,0); d(0,0,1); d(1,1,0); d(0,1,1);

d(1,0,1); d(3,3,3); d(3,0,0); d(0,3,0); d(0,0,3); d(3,3,0); d(0,3,3); d(3,0,3). By doing so the total volume of pixels needed for the calculation is 18x18x18 (i.e. cube size plus one of the above directions). The final number of characteristics is 168 (8 characteristics x 7 angle directions x 1 cube size + 14 angle directions x 1 cube size). By applying a PCA, the total number is reduced to 3. This final result is selected for the number of clusters to be assigned for the *k*-means analysis. The border is afterward found on the segmented polar image and transformed back into the original image format. The method was tested on three patient databases that included 4 IVUS sequences, each one having approximately 3000 images, of which 75 images were analyzed.

3 Results & Discussion

Initially, before the IVUS images are transformed to polar coordinates, secondary artifacts like calibration markers should be removed. Unfortunately the transformation to polar coordinates reduces the quality of the images. Hence to alleviate this problem as much as possible, the polar images were sized to 240 X 360 pixels.

The second phase consists of extracting the characteristics of the images using the 3D co-occurrence matrices. This process takes several minutes per image on a P4 2.6 Ghz computer, implemented in C++. Since this first preprocessing step is very time-consuming, it is necessary to choose strategically the total number of characteristics for the 3D co-occurrence matrix and k-means analysis. The chosen cube size is of primary importance as it is not possible to extract all the characteristics on all the IVUS sequence as seen in Figure 3b. Based on a priori testing with different cube sizes, the 9x9x9 and 17x17x17 sizes were selected as they contain enough image texture information without being hindered by possible artifacts such as noise or motion. The methodology was modified to reduce computing time. First, the characteristics are extracted only at 4º intervals and an inter-frame interpolation was carried out to complete the missing data. Secondly, a maximum limit for the value of the radius *r* can be given as the lumen does not span the entire image. With respect to the direction, it is necessary to choose orientations which cover the entire space uniformly. In this case, we deemed that the main 7 directions (major axes and corner diagonals) are sufficient for the analysis. The dimension of the direction is also important since we need to consider the edge *(see figure 4b)*. A dimension equal to 1 was chosen for the 17x17x17 cube and a dimension equal to 1 and 3 was assigned for the 9x9x9 cube. Because of that, 9 pixels are lost on the top and bottom of the image analyzed and the first 9 images at the beginning and end of the sequence are not used for the analysis.

The third step consists in the reduction of the features space. The PCA algorithm reduced the features space to three so as to remove the correlation between the characteristics and to reduce the redundancy of information (*see figure 5*). The algorithm keeps approximately 85% of the information given by the 168 characteristics. Hence, each pixel of the image has 3 characteristics.

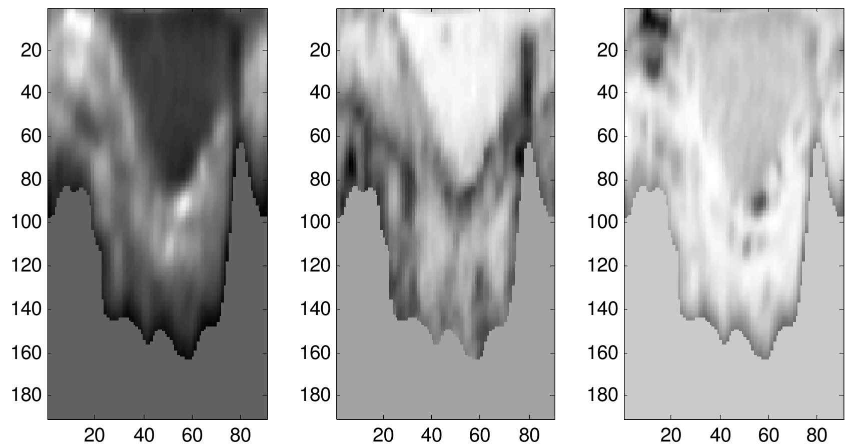

Fig.5. The three characteristics images obtained after the PCA space reduction (ordered from left to right).

The fourth phase consists in the classification of the pixels. Pixels classification in the characteristic space was fed into the *k*-means classifier with 3 centers. A significant problem with this algorithm is that the representative distribution obtained is usually large. To remedy this, image subsections or patches which do not contain relevant texture information must be removed. In order to do this, a binary mask representing the chosen pixels was created (*see figure 6a*). If the region of the mask is black, then the associated pixels are not used as input for the classifier. The mask is formed by creating 5 horizontal white bands (~20% of the image) on a black background. The characteristic energy of the co-occurrence matrices is subtracted from the mask. This signifies that the uniform texture regions contained in every IVUS image is not included during the classification stage. This is not a problem for the analysis as the uniform region is usually located at the bottom of the polar image, whereas the borders of interest are located at the top of the polar image. Some of the lumen and vessel tissue pixels were still fed into the classifier so that the classification was more accurate (*see figure 6b*). Although the choice of the initial centers for the *k*-means classifier is important, they can be chosen randomly because the *k*-means algorithm does not remain trapped in local minima as explained in the previous section. Once the three cluster centers were found, the pixels were associated to the nearest center. The two vessel clusters were merged to obtain only two classes because the clusters belonging to the vessel structure have a larger standard deviation than the lumen. The lumen cluster is smaller than the intima, media and adventitia clusters, because its pixels represent only one tissue. Sometimes the adventitia has a similar texture as the lumen. This is not a problem since we want to find the border between the lumen and the intima and so the adventitia has no influence on this final border. The unclassified pixels are determined by applying a threshold of 20% of the minimal distance between the lumen cluster and the vessel clusters. After the classification, a segmentation image was created. This image has two classes, the lumen and the vessels. The image includes also some uncertain pixels which are between the classes (*see figure 6d*).

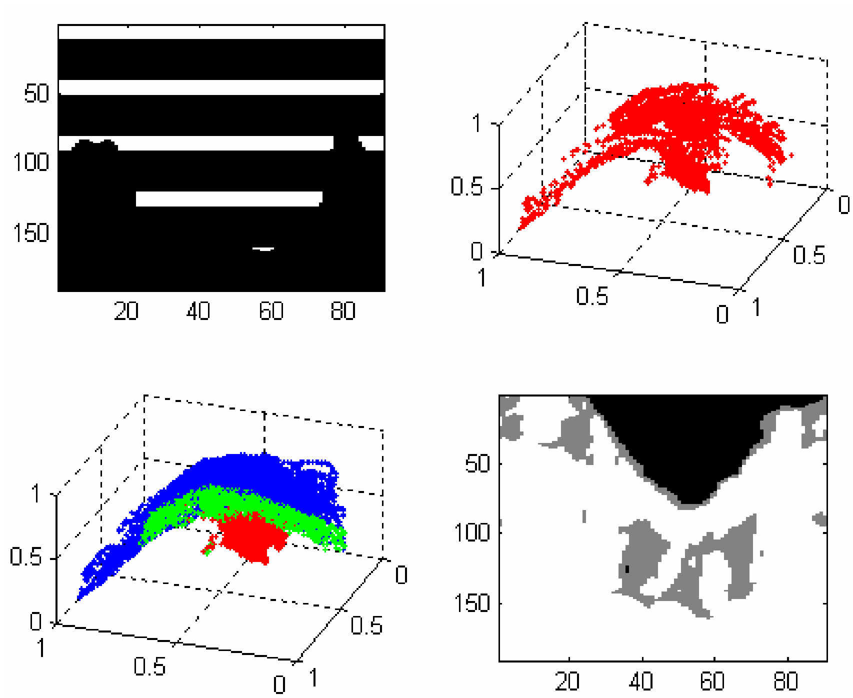

Fig. 6. (*a top-left*) The feature space image mask; in white the pixels that are given to the classifier. (*b top-right*) the distribution that is given to the *k*-means classifier. (*c bottom-left*) The 3 cluster given by the classifier. The front distribution is representing the lumen, the far distribution is representing the vessel and the uncertain is located between them. (*g bottom-right*) the segmentation image that incorporates the lumen class in black, the vessel tissue class in white and the unclassified pixels in gray.

The last phase consists in finding the separation border between the classes by also considering the unclassified pixels. The border has to pass through the center of the uncertain area. Once the border was identified, it was processed using a Gaussian smoothing filter. The border was then scaled back onto the original IVUS image by using a cubic interpolation. It is necessary to consider the angle sampling and the radius trim. All of the transformations presented in the methodology introduce several approximation errors in the order of a few pixels. The lumen-intima border found on the IVUS images by our method (*see figure 7 right*) is close to the border identified by an expert (*see figure 7 left*).

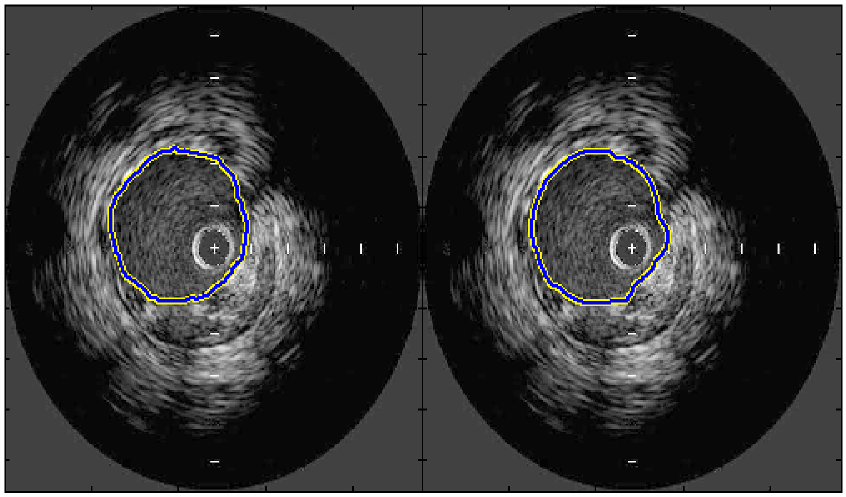

Fig. 7. *(left)* The lumen-intima border identified manually and (*right*) determined by the proposed method.

Results show that 80% of the 300 total IVUS images used in the analysis are partially or correctly segmented. This means that 70% of the lumen contour border is segmented properly with a few minor gaps. The remaining 20% of the images aren't correctly segmented, because the texture in the lumen and the vessel are very similar and the algorithm can't find any separation between them. The identification of the two vessel clusters can produce some errors by associating the lumen cluster to the vessel and by identifying one of the vessel clusters as the lumen.

As most IVUS images are difficult to segment manually by an expert, we believe the results obtained from our proposed method will speed up the segmentation process. Furthermore, the gaps seen in some of the borders are created by the guidewire echo or because the catheter touches the intima. Imperfections also arise when there are vessel bifurcations in the IVUS images or when the lumen-intima border is too convex.

Future work should focus on the removal of the echo created by the guidewire. Co-occurrence matrices are a powerful texture operator but the parameters must be found experimentally. Tests could be carried on by choosing other cube sizes, other orientations or even other characteristics. The *k*-means classifier could be used with more than 3 classes to possibly identify the border between the media and the adventitia.

4 Conclusion

The method suggested in this paper is a new approach for IVUS image segmentation, specifically targeting poor quality images. Automatic identification of the lumen-intima border is effective on the majority of the IVUS images, in spite of significant noise present in most of them. The 3D co-occurrence matrices take into account the spatiotemporal texture information in the IVUS sequence. By using a *k*-means classifier we can segment the images without any training phase or prior knowledge. The full characterization of the morphology of the vessel is the future prospect for this method.

References

1. M. Olszewski, A. Wahle, S. Vigmostad, M. Sonka "Multidimensional segmentation of coronary intravascular ultrasound images using knowledge-based methods", Medical Imaging 2005: Image Processing. Edited by Fitzpatrick, J. Michael; Reinhardt, Joseph M. Proceedings of the SPIE, Volume 5747, 2005, pp. 496-504.
2. M.R. Cardinal, J. Meunier, G. Soulez, E. Therasse, G. Cloutier, "Intravascular Ultrasound Image Segmentation: A Fast-Marching Method", Medical Image Computing and Computer-Assisted Intervention – MICCAI, 2003, pp. 432-439.
3. M.R. Cardinal, J. Meunier, G. Soulez, E. Therasse, G. Cloutier, "Automatic 3D Segmentation of Intravascular Ultrasound Images Using Region and Contour Information", Medical Image Computing and Computer-Assisted Intervention – MICCAI, 2005, pp. 319-326.
4. O. Pujol, D. Rotger, P. Radeva, O. Rodriguez, J. Mauri, "Near real-time plaque segmentation of IVUS", Computers in Cardiology, 2003 Volume, pp 66-72.
5. O. Pujol, P. Radeva, "On the assessment of texture feature descriptors in intravascular ultrasound images: A boosting approach to a feasible plaque classification", Plaque Imaging: Pixel to Molecular Book, 2005, pp. 276-299.
6. O.Pujol, P. Radeva, "Lumen detection in IVUS images using snakes in a statistical framework", Congreso Anual de la Sociedad Española de Ingeniería Biomédica, Zaragoza, 2002..
7. E. Brunenberg, O. Pujol, B. Romeny, P. Radeva, "Automatic IVUS Segmentation of Atherosclerotic Plaque with Stop & Go Snake", Medical Image Computing and Computer-Assisted Intervention – MICCAI. 2006, pp. 9-16.
8. E. Santos Filho, M. Yoshizawa, A, Tanaka, Y. Saijo, T. Iwamoto, "Moment-based texture segmentation of luminal contour in intravascular ultrasound images", Journal of Medical Ultrasonics, 2005, pp.91-99.
9. A.Kurani, H.-H. Xu, J. Fustm D. Raicu, "Co-occurrence Matrices for Volumetric Data", Computer Graphics and Imaging, 2004, 426-085.
11. T. Kanungo, D. Mount, N. Netanyahu, C. Piatkpo, R. Silverman, A.Y. Wu, "An efficient k-means clustering algorithm: Analysis and implementation", IEEE Trans. Pattern Analysis and Machine Intelligence, 2002, pp. 881-892.
12. T. Kanungo, D. Mount, N. Netanyahu, C. Piatkpo, R. Silverman, A.Y. Wu,. "A Local Search Approximation Algorithm for k-Means Clustering", Computational Geometry: Theory and Applications, 2004, pp. 89-112.
13. R. Haralick, K. Shabmugam, I. Dinstein, "Textural Features for image classification", IEEE transactions on systems and cybernetics, Vol. 3, 1973, pp. 610-621.
14. R. Duda, P. Hart, D. Stork, "Pattern Classifications", Wiley-Interscience Publication 2001, 654 pages.
15. RC. Gonzales, RE Woord, "Digital image processing 2nd Edition", Upper saddle river,N.J.: Prentice Hall 2002, 793 pages.
16. M. Kass, A. Witkin, D. Terzepoulos, "Snakes: Active contour models", International Journal of Computer Vision, Vol.1 No. 4, 1987, pp. 321-331.